

Determination of Scalar Coupling Constants by Inverse Fourier Transformation of In-Phase Multiplets

T. SZYPERSKI, P. GÜNTERT, G. OTTING, AND K. WÜTHRICH

Institut für Molekularbiologie und Biophysik, Eidgenössische Technische Hochschule-Hönggerberg, CH-8093 Zurich, Switzerland

Received December 17, 1991

A generally applicable new method for the determination of scalar coupling constants for spins with a single coupling partner, in particular $^3J_{\text{HN}\alpha}$ in polypeptides, is described. It has the special advantage for use in protein structure determinations that no extra NMR experiments need to be recorded, and that NOE distance constraints and dihedral angle constraints from $^3J_{\text{HN}\alpha}$ can be derived from the same data sets. The scalar coupling constants are extracted from the in-phase multiplets of homonuclear [^1H , ^1H] NOESY spectra or heteronuclear [^{15}N , ^1H] COSY spectra through inverse Fourier transformation of the data points representing a cross peak along ω_2 , and a subsequent nonlinear least-squares fit in the time domain. Practical applications are described for recombinant hirudin and the basic pancreatic trypsin inhibitor. © 1992 Academic Press, Inc.

Besides ^1H - ^1H NOEs, vicinal coupling constants provide the most important information for a protein structure determination by NMR (1). In particular, $^3J_{\text{HN}\alpha}$ coupling constants in peptides and proteins provide experimental constraints for the backbone dihedral angle ϕ (2-4) and provide essential information for obtaining stereospecific assignments for pairs of diastereotopic protons (5, 6). In principle, $^3J_{\text{HN}\alpha}$ coupling constants can be measured in a straightforward manner from the separation of the components in antiphase doublets in [^1H , ^1H] COSY (7, 8). However, the linewidth of proton resonances in proteins is often comparable to or even larger than the scalar coupling constants, resulting in partial cancellation of the antiphase multiplet components. This reduces the overall peak intensity and increases the separation of the components observed in the COSY cross peaks, leading to a systematic artifactual overestimation of those coupling constants which are small relative to the linewidth (9). Recently, several methods have been developed to overcome this problem, all using ^{15}N -labeled proteins (10-12). In the present paper we propose to determine $^3J_{\text{HN}\alpha}$ coupling constants from in-phase doublets by inverse Fourier transformation, since in-phase doublets are often more readily available with good signal-to-noise ratios than antiphase doublets. The method focuses primarily on [^1H , ^1H] NOESY spectra, which are routinely recorded with a good signal-to-noise ratio to collect NOE distance constraints for the determination of the three-dimensional structure of proteins (1). All conformational constraints used for the structure determination can then be derived from a single experimental data set. Alternatively, if a ^{15}N -labeled protein is

available, proton-detected heteronuclear [^{15}N , ^1H] COSY can be used for the data collection.

Practical applications of the currently proposed method are illustrated with two proteins, and the results obtained are compared with corresponding data collected with standard techniques. For the N-terminal 51-residue domain of recombinant Hirudin¹ the coupling constants measured in a 2QF-COSY spectrum were compared to those extracted by inverse FT from a [^1H , ^1H] NOESY spectrum. For the basic pancreatic trypsin inhibitor (BPTI, 58 residues) the coupling constants extracted by inverse FT from the [^1H , ^1H] NOESY spectrum that was recorded to collect NOE constraints for the structure determination (13) were compared with the values determined using the ^{15}N -enriched protein, either for J -modulated [^{15}N , ^1H] COSY (12, 20) or for inverse FT of a proton-detected [^{15}N , ^1H] COSY spectrum.

METHODS

Determination of $^3J_{\text{HN}\alpha}$ coupling constants from [^1H , ^1H] NOESY spectra. In a [^1H , ^1H] NOESY experiment all cross peaks at the ω_2 frequency of a given proton show the same in-phase multiplet fine structure along ω_2 . In particular, for an amide proton of a nonglycine α -amino acid residue, a doublet is observed due to the scalar coupling with the α proton, which results in a simple $\cos(\pi J_{\text{HN}\alpha}t)$ dependence of the signal detected during the acquisition period. Since more than one NOE is usually observed for each amide proton, the analysis of this doublet fine structure in NOESY spectra is much less limited by spectral overlap than in [^1H , ^1H] COSY spectra. In addition, two or several cross sections along the ω_2 frequency axis which belong to resolved cross peaks with a given amide proton may be added in order to improve the signal-to-noise ratio for the determination of the $^3J_{\text{HN}\alpha}$ coupling constant. Thereby, since the lineshape of NOESY cross peaks between scalar-coupled protons is often affected by some J -cross-peak contribution (14, 15), intraresidual C^αH -NH NOESY cross peaks should not be included for the determination of the $^3J_{\text{HN}\alpha}$ coupling constants.

To determine the $^3J_{\text{HN}\alpha}$ coupling constant for a given residue, one or several well-separated NOESY cross peaks with the backbone amide proton in the ω_2 dimension are used (Fig. 1a). Several cross sections through these cross peaks are selected that exhibit a good signal-to-noise ratio. These are added up and only those data points of the peak region are retained that are above the noise level (Fig. 1b). The left and right ends of the peak region are then brought to zero intensity by a linear baseline correction. After extending the baseline-corrected peak region with zeros on both sides, which is equivalent to oversampling in the time domain, an inverse FT is performed. The zero point in the frequency domain is chosen about 1000 Hz away from the peak considered, so that the modulation of the time-domain signal by the scalar couplings is not disturbed by an unwanted additional modulation which would arise if the zero point were set near to, but not exactly at the center of, the peak. From this envelope of the time-domain signal after inverse FT (Fig. 1c) a first estimate, $J^{(0)}$, for the value of the $^3J_{\text{HN}\alpha}$ coupling constant is obtained from the first local minimum, which is ideally defined

¹ Abbreviations used: Hirudin(1-51), N-terminal 51-residue polypeptide from recombinant Hirudin of the leech *Hirudo medicinalis*; 2QF, two-quantum filtered.

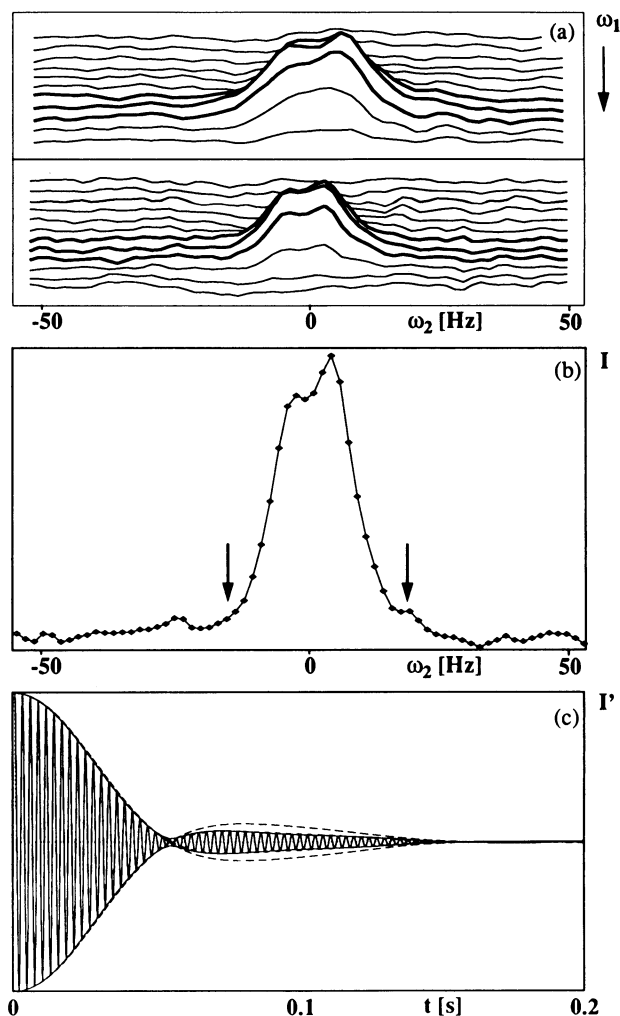


FIG. 1. Illustration of the procedure used to determine $^3J_{\text{HN}\alpha}$ coupling constants by inverse FT. The intraresidual NOEs from the two diastereotopic β protons to the amide proton of Cys 22 in Hirudin(1-51) are shown. (a) Stacked plot of the two ^1H , ^1H NOESY cross peaks, with the amide proton of Cys 22 along ω_2 . The rows plotted with bold lines were selected for further processing. (b) Intensity, I , of the sum of the six rows plotted with bold lines in (a). The peak region used for further processing is bounded by two vertical arrows. (c) Time-domain signal obtained by inverse FT of the peak region in (b). Also drawn are the envelope of this time-domain signal (smooth, solid line), the envelope of the time-domain signal corresponding to the initial estimates for the coupling constant and the linewidth (broken line), and the envelope of the time-domain signal corresponding to the final, best-fit of the coupling constant and the linewidth (broken line that nearly coincides with the solid line over the entire time range). Note the nonexponential shape of the FIDs, which is due to the convolution with a sinc function (see text for further details).

by a zero crossing. An initial estimate for the linewidth, $\Gamma^{(0)}$, is then obtained by measuring the full width at half-height, $\Delta\nu_{1/2}$, of the peak in the frequency domain, using that $\Gamma^{(0)} = \Delta\nu_{1/2} - J^{(0)}$. These initial estimates for the coupling constant and the linewidth are iteratively refined using a nonlinear least-squares fit (Levenberg–Marquardt algorithm (16)) that minimizes the squared deviation between the envelope obtained from the experimental data and the simulated envelope corresponding to $J^{(0)}$ and $\Gamma^{(0)}$. In the simulation of the envelope after inverse FT, care must be taken to account for effects caused by the discrete FT, by the filter functions used, by zero-filling, and in particular by cutting the comparably small peak region out of the spectrum. This cutting procedure is equivalent to a multiplication of the peak with a step function that equals unity within the peak region and vanishes outside. According to the convolution theorem this leads to a convolution of the FID with a sinc function. Because the convolution integral containing the sinc function cannot be solved analytically, the envelope must be simulated by repeating all the steps of the procedure that was used to obtain the envelope from the experimental data: Assuming relaxation with a single exponential decay, the envelope of the FID recorded for an in-phase doublet is given by

$$S(t) = \cos(\pi J_{\text{HN}\alpha} t) e^{-\pi \Gamma t}, \quad 0 \leq t \leq t_{\text{aq}}, \quad [1]$$

where t_{aq} denotes the experimental acquisition time. Starting from $S(t)$ of Eq. [1], identical filter functions and zero-filling as for the experimental data are applied. The result is subjected to a discrete FT and the peak obtained is treated in the same way as described above for the experimental peak. Finally, a discrete inverse FT is used to obtain the simulated envelope, which can be compared to the corresponding envelope obtained from the experimental spectrum.

For the Levenberg–Marquardt algorithm used to calculate the nonlinear fit, the gradient of the simulated envelope after inverse FT with respect to the coupling constant and the linewidth is needed. This gradient can readily be obtained because the formation of partial derivatives with respect to the coupling constant and the linewidth commutes with all the operations that lead from the envelope $S(t)$ of Eq. [1] to the simulated envelope after inverse FT. Therefore, the desired gradient can be computed analytically by applying to the partial derivatives of $S(t)$ the same procedure that had yielded the simulated envelope after inverse FT.

Determination of $^3J_{\text{HN}\alpha}$ coupling constants from [^{15}N , ^1H] COSY spectra. The ^1H -detected [^{15}N , ^1H] COSY experiment of Bodenhausen and Ruben (17) is the most sensitive 2D NMR experiment for detection of the amide proton resonances in ^{15}N -enriched proteins. The experimental scheme of Fig. 2 differs from the original experiment by the presence of a $(\pi/2)(^1\text{H})$ pulse before the detection period, which removes undesired dispersive contributions from the ^{15}N – ^1H cross peak. The effect of this purge pulse is apparent from a product-operator description (18). Denoting the ^{15}N spin with N, the amide proton with H^{N} , and the α proton with H^{α} , we have at the beginning of the second delay τ (Fig. 2) heteronuclear antiphase magnetization $2\text{H}_y\text{N}_z$. This term evolves during τ under the scalar coupling Hamiltonian with respect to the heteronuclear coupling $^1J[^1\text{H}, ^{15}\text{N}]$ as well as the homonuclear coupling $^3J_{\text{HN}\alpha}$:

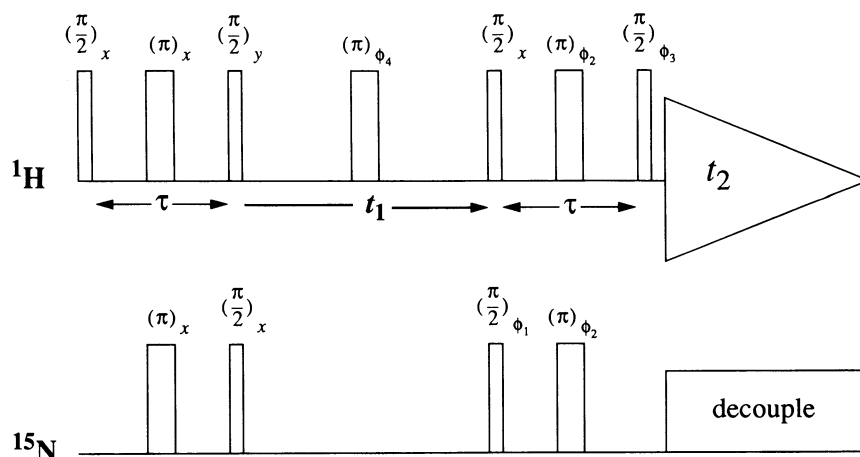


FIG. 2. Modified experimental scheme for [^{15}N , ^1H] COSY that yields undistorted in-phase doublets along ω_2 for the determination of $^3J_{\text{HN}\alpha}$ coupling constants with Eq. [1]. The delay τ is tuned to $\frac{1}{2}[^1J(^1\text{H}, ^{15}\text{N})]$. The phase cycle is $\phi_1 = 8(x, -x)$, $\phi_2 = 4(x, x, -x, -x)$, $\phi_3 = 2(x, x, x, x, -x, -x, -x, -x)$, $\phi_4 = 8(x), 8(-x)$, receiver = $8(x, -x)$. In addition, all phases may be incremented in 90° steps to suppress quadrature images (CYCLOPS). Quadrature detection along ω_1 is achieved by subjecting the first two ^{15}N pulses to time-proportional phase incrementation (TPPI) (7). Decoupling during acquisition is achieved using a WALTZ-16 sequence (24).

$$2\text{H}_y^{\text{N}}\text{N}_z^{\text{N}} \xrightarrow{\tau/2 - \pi\phi_2 - \tau/2} \text{H}_x^{\text{N}} \cos(\pi J_{\text{HN}\alpha}\tau) \sin(\pi ^1J[^1\text{H}, ^{15}\text{N}]\tau) + 2\text{H}_y^{\text{N}}\text{H}_z^{\alpha} \sin(\pi J_{\text{HN}\alpha}\tau) \sin(\pi ^1J[^1\text{H}, ^{15}\text{N}]\tau). \quad [2]$$

On the right-hand side of Eq. [2] all heteronuclear coherences in antiphase with respect to the ^{15}N spin were omitted, since they are destroyed by ^{15}N decoupling during detection (Fig. 2). The magnetization H_x^{N} is in-phase with respect to $^3J_{\text{HN}\alpha}$ and evolves during the detection period, t_2 , with the same $\cos(\pi J_{\text{HN}\alpha}t_2)$ dependence as the amide proton magnetization in a [^1H , ^1H] NOESY experiment (Eq. [1]). The magnetization $2\text{H}_y^{\text{N}}\text{H}_z^{\alpha}$ of Eq. [2] would be antiphase with respect to $^3J_{\text{HN}\alpha}$ and 90° out of phase with respect to the term H_x^{N} . In the experimental scheme of Fig. 2 the $(\pi/2)$ (^1H) purge pulse before the detection period converts this undesired dispersive contribution into $2\text{H}_z^{\text{N}}\text{H}_y^{\alpha}$, which represents magnetization precessing at the α -proton chemical shift during the detection period. In this way pure in-phase absorptive lineshapes are obtained for the amide proton multiplets, which can be evaluated with the same procedure as described above for NOESY (Eq. [1]). Alternatively, the original, unmodified experimental scheme of Bodenhausen and Ruben (17) could be used, provided that the dispersive antiphase magnetization is accounted for in the fitting procedure. The envelope of the recorded signal, $S(t)$, would then be given by

$$S(t) = [\cos(\pi J_{\text{HN}\alpha}\tau) \cos(\pi J_{\text{HN}\alpha}t) - \sin(\pi J_{\text{HN}\alpha}\tau) \sin(\pi J_{\text{HN}\alpha}t)] e^{-\pi\Gamma t}. \quad [3]$$

The $^3J_{\text{HN}\alpha}$ coupling constants thus obtained are of comparable accuracy to those determined using the experiment of Fig. 2 and Eq. [1]. It should be noted that the

use of a spin-lock purge pulse in this experiment (19) leads to further unwarranted terms during the detection period, which need to be accounted for in the fitting procedure used to obtain the ${}^3J_{\text{HN}\alpha}$ coupling constants.

RESULTS

In this section the results of ${}^3J_{\text{HN}\alpha}$ measurements using inverse Fourier transformation of $[{}^1\text{H}, {}^1\text{H}]$ NOESY or $[{}^{15}\text{N}, {}^1\text{H}]$ COSY are compared with corresponding results obtained with different techniques.

Hirudin(1-51). All coupling constants extracted by inverse FT from a $[{}^1\text{H}, {}^1\text{H}]$ NOESY spectrum were found to be smaller than those obtained by measurements of the antiphase peak separation in a 2QF-COSY spectrum. These systematic differences are mainly due to partial peak cancellation in the 2QF-COSY spectrum, as is clearly evidenced by the plot of ${}^3J(\text{COSY})/\Gamma(\text{NOE})$ against ${}^3J(\text{NOE})/\Gamma(\text{NOE})$ in Fig. 3, where the experimental data points follow the curve representing the simulated relationship of the two coefficients expected for Lorentzian lineshapes (9). The systematic errors in the coupling constants measured in the COSY spectrum could not readily

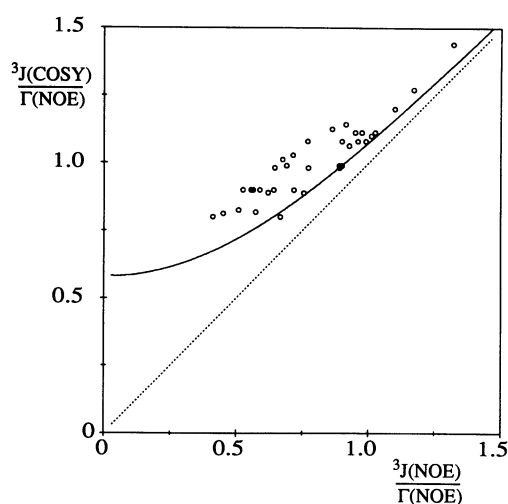


FIG. 3. Comparison of the coupling constant-to-linewidth ratios ${}^3J(\text{COSY})/\Gamma(\text{NOE})$ and ${}^3J(\text{NOE})/\Gamma(\text{NOE})$ obtained for Hirudin(1-51). ${}^3J(\text{COSY})$ are the ${}^3J_{\text{HN}\alpha}$ values obtained from the separation of the antiphase peaks in homonuclear 2QF-COSY, the ${}^3J(\text{NOE})$ s are those obtained from inverse FT of $[{}^1\text{H}, {}^1\text{H}]$ NOESY, and $\Gamma(\text{NOE})$ denotes the linewidth obtained in the fit of the NOESY spectrum (Eq. [1]). The solid curve represents the relationship between the two quantities simulated with the assumption of Lorentzian lineshapes (9). The experimental data are given by the circles. For both spectra the ${}^1\text{H}$ frequency was 600 MHz, $T = 22^\circ\text{C}$, and the solvent was 90% $\text{H}_2\text{O}/10\% \text{D}_2\text{O}$. For the 2QF-COSY spectrum the data size was 1100×4096 points, $t_{1\text{max}} = 75$ ms, $t_{2\text{max}} = 279$ ms, and 16 scans per t_1 increment were recorded. For NOESY the data size was 960×4096 points, $t_{1\text{max}} = 65$ ms, $t_{2\text{max}} = 279$ ms, and 128 scans per t_1 increment were recorded. The spectra were zero-filled along t_2 to 16K and 8K data points, respectively, to yield a digital resolution of 0.9 and 1.8 Hz along ω_2 . Before FT the data were multiplied with a sine-bell window shifted by $\pi/2$ (25).

be corrected on the basis of the COSY data alone, since the linewidths would not be known with sufficient precision.

Basic pancreatic trypsin inhibitor. The scalar coupling constants $^3J_{\text{HN}\alpha}$ for unlabeled BPTI were obtained by inverse FT from a [^1H , ^1H] NOESY spectrum. For ^{15}N -enriched BPTI, corresponding data resulted from a [^{15}N , ^1H] COSY spectrum by inverse FT and, independently, from analysis of a series of J -modulated [^{15}N , ^1H] COSY spectra (12, 20). The data are presented in Fig. 4. The plot of Fig. 4a compares the $^3J_{\text{HN}\alpha}$ values obtained by inverse FT of a [^{15}N , ^1H] COSY experiment recorded with the scheme of Fig. 2, or a [^1H , ^1H] NOESY experiment, respectively. The root mean square deviation (RMSD) between the two sets of coupling constants was determined to be 0.22 Hz. In Fig. 4b the values extracted by inverse FT from the [^1H , ^1H] NOESY spectrum are compared to those obtained from a series of J -modulated [^{15}N , ^1H] COSY experiments (12, 20). The RMSD between the two sets of coupling constants was determined to be 0.32 Hz, showing that the results obtained with the two methods are in excellent agreement. Finally, a [^{15}N , ^1H] COSY spectrum was recorded without the final 90° pulse on the protons (Fig. 2), and the ensuing systematic distortion of the lineshapes was accounted for by using Eq. [3] for the fitting procedure. The resulting $^3J_{\text{HN}\alpha}$ values were again compared to the values obtained from inverse FT of the [^1H , ^1H] NOESY spectrum, and a RMSD of 0.38 Hz was calculated (data not shown). This shows that using the original, unmodified experimental scheme for [^{15}N , ^1H] COSY combined with the data analysis using Eq. [3] is a valid alternative to the use of the optimized experiment of Fig. 2 for the purpose of $^3J_{\text{HN}\alpha}$ measurements with inverse FT.

DISCUSSION

The main advantages of the $^3J_{\text{HN}\alpha}$ measurements by inverse FT of [^1H , ^1H] NOESY are the high efficiency and the fact that all input data for the structure determination can be obtained from the same data set. [^1H , ^1H] NOESY spectra must be recorded routinely during the course of a protein structure determination and the fitting procedure with Eq. [1] is fast, requiring a few CPU seconds on a Sun4 workstation. Currently, the fitting procedure is implemented in the program INFIT (available from the authors). Planned implementation into the *ETH automated spectroscopy* (EASY) program package (21) will allow a fully automated extraction of coupling constants from spectra with in-phase multiplets.

The precision of the method is comparable to the precision reached using a series of J -modulated [^{15}N , ^1H] COSY spectra. One advantage of using a series of J -modulated [^{15}N , ^1H] COSY spectra may be that the refocusing 180° pulse during the evolution of the homonuclear $^3J_{\text{HN}\alpha}$ coupling (12) refocuses magnetic field inhomogeneities. However, relatively long measurement times are required with the J -modulated [^{15}N , ^1H] COSY technique, and as for other recently published methods (10, 11, 22) ^{15}N labeling is required. Another method which does not require ^{15}N labeling has been proposed, which uses a combination of [^1H , ^1H] NOESY and [^1H , ^1H] COSY spectra to extract $^3J_{\text{HN}\alpha}$ coupling constants (23). Although this method avoids the overestimation of coupling constants due to mutual cancellation, it is still limited by the loss of intensity in the [^1H , ^1H] COSY spectra arising from mutual cancellation.

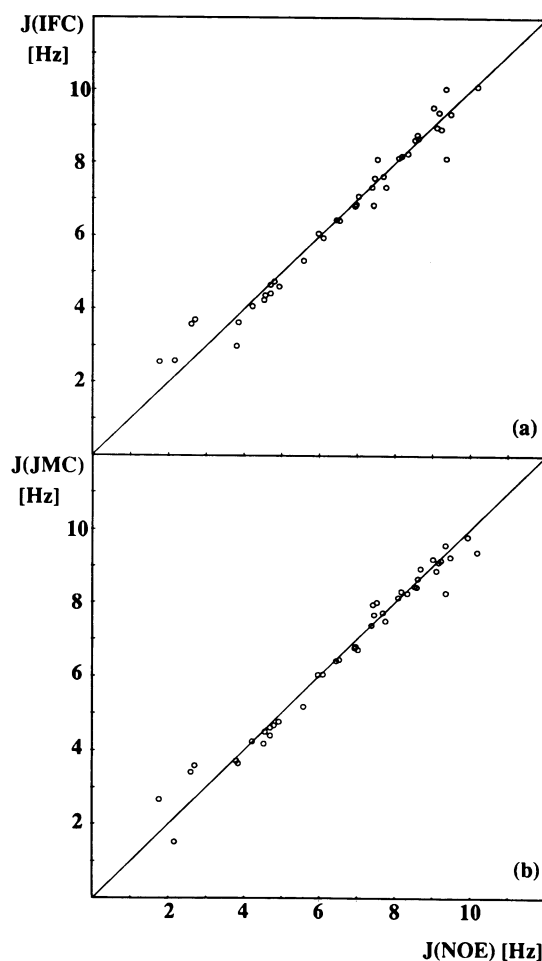


FIG. 4. Comparison of amide proton- α -proton coupling constants for BPTI obtained from a [^1H , ^1H] NOESY spectrum by inverse FT and a fit with Eq. [1], $J(\text{NOE})$, to corresponding data obtained with the following different procedures: (a) [^{15}N , ^1H] COSY recorded with the scheme of Fig. 2, inverse FT, and the fitting procedure of Eq. [1], $J(\text{IFC})$. (b) Analysis of a series of J -modulated [^{15}N , ^1H] COSY spectra with the procedures of Billeter *et al.* (20), $J(\text{JMC})$. For all three experiments the protein concentration was 10 mM, $T = 36^\circ\text{C}$, and the solvent was 90% H_2O /10% D_2O , pH 4.6. For NOESY the ^1H frequency was 600 MHz, the data size was 512×4096 points, $t_{1\text{max}} = 32$ ms, $t_{2\text{max}} = 254$ ms, 192 scans per t_1 increment were recorded, zero-filling was used to 8192 points in t_2 , the digital resolution in ω_2 was 1.9 Hz, and filtering was with a $\pi/2$ shifted sine bell (25). For [^{15}N , ^1H] COSY used for obtaining $J(\text{IFC})$, the ^1H frequency was 500 MHz, the data size was 212×3072 points, $t_{1\text{max}} = 29$ ms, $t_{2\text{max}} = 246$ ms, 8 scans per t_1 increment were recorded, zero-filling was to 8192 points in t_2 , the digital resolution was 1.5 Hz, and filtering was with a $\pi/2$ shifted sine bell. Sixteen [^{15}N , ^1H] COSY spectra for $J(\text{JMC})$ were recorded at a ^1H frequency of 500 MHz, the data size was 160×2048 points, $t_{1\text{max}} = 61$ ms, $t_{2\text{max}} = 160$ ms, and 64 scans per t_1 increment were recorded.

Another limitation of this procedure arises whenever overlap occurs in the fingerprint region.

Finally it should be added that the inverse FT approach presented here can be used in a straightforward manner in three-dimensional experiments which yield in-phase doublets along the ω_3 frequency axis.

ACKNOWLEDGMENTS

Financial support was obtained from the Schweizerischer Nationalfonds (Project 31.25174.88) and the Stipendien-Fonds im Verband der Chemischen Industrie (fellowship to T.S.). We thank Bayer AG, Leverkusen, Germany, for a generous gift of ^{15}N -enriched BPTI, Dr. L. P. M. Orbons for recording the J -modulated [^{15}N , ^1H] COSY data of BPTI, and Mr. R. Marani for the careful processing of the manuscript.

REFERENCES

1. K. WÜTHRICH, "NMR of Proteins and Nucleic Acids," Wiley, New York, 1986.
2. M. KARPLUS, *J. Am. Chem. Soc.* **85**, 2870 (1963).
3. V. F. BYSTROV, *Prog. NMR Spectrosc.* **10**, 41 (1976).
4. A. PARDI, M. BILLETER, AND K. WÜTHRICH, *J. Mol. Biol.* **180**, 741 (1984).
5. P. GÜNTERT, W. BRAUN, M. BILLETER, AND K. WÜTHRICH, *J. Am. Chem. Soc.* **111**, 3997 (1989).
6. P. C. DRISCOLL, A. M. GRONENBORN, AND G. M. CLORE, *FEBS Lett.* **243**, 223 (1989).
7. D. MARION AND K. WÜTHRICH, *Biochem. Biophys. Res. Commun.* **113**, 967 (1983).
8. H. KESSLER, M. GEHRKE, AND C. GRIESINGER, *Angew. Chem. Int. Ed. Engl.* **27**, 490 (1988).
9. D. NEUHAUS, G. WAGNER, M. VAŠÁK, J. H. R. KÄGI, AND K. WÜTHRICH, *Eur. J. Biochem.* **151**, 257 (1985).
10. G. T. MONTELIONE AND G. WAGNER, *J. Am. Chem. Soc.* **111**, 5474 (1989).
11. L. E. KAY, B. BROOKS, S. W. SPARKS, D. A. TORCHIA, AND A. BAX, *J. Am. Chem. Soc.* **111**, 5488 (1989).
12. D. NERI, G. OTTING, AND K. WÜTHRICH, *J. Am. Chem. Soc.* **112**, 3663 (1990).
13. K. BERNDT, P. GÜNTERT, L. P. M. ORBONS, AND K. WÜTHRICH, *J. Mol. Biol.*, in press.
14. S. MACURA, Y. HUANG, D. SUTER, AND R. R. ERNST, *J. Magn. Reson.* **43**, 259 (1981).
15. M. RANCE, G. BODENHAUSEN, G. WAGNER, K. WÜTHRICH, AND R. R. ERNST, *J. Magn. Reson.* **62**, 497 (1985).
16. W. H. PRESS, B. P. FLANNERY, S. A. TEUKOLSKY, AND W. T. VETTERLING, "Numerical Recipes," Cambridge Univ. Press, Cambridge, 1986.
17. G. BODENHAUSEN AND D. J. RUBEN, *Chem. Phys. Lett.* **69**, 185 (1980).
18. O. W. SØRENSEN, G. W. EICH, M. H. LEVITT, G. BODENHAUSEN, AND R. R. ERNST, *Prog. NMR Spectrosc.* **16**, 163 (1983).
19. G. OTTING AND K. WÜTHRICH, *J. Magn. Reson.* **76**, 569 (1988).
20. M. BILLETER, D. NERI, G. OTTING, Y. Q. QIAN, AND K. WÜTHRICH, *J. Biomol. NMR* **2**, 257 (1992).
21. C. ECCLES, P. GÜNTERT, M. BILLETER, AND K. WÜTHRICH, *J. Biomol. NMR* **1**, 111 (1991).
22. O. W. SØRENSEN, *J. Magn. Reson.* **90**, 433 (1990).
23. S. LUDVIGSEN, K. V. ANDERSEN, AND F. M. POULSEN, *J. Mol. Biol.* **217**, 731 (1991).
24. A. J. SHAKA, J. KEELER, AND R. FREEMAN, *J. Magn. Reson.* **53**, 313 (1983).
25. A. DE MARCO AND K. WÜTHRICH, *J. Magn. Reson.* **24**, 201 (1976).